Kinetics of Aqueous Phase Dehydration of Xylose into Furfural Catalyzed by ZSM-5 Zeolite

Kinetics of Aqueous Phase Dehydration of Xylose into Furfural Catalyzed by ZSM-5 Zeolite

Rebecca O'Neill, Mohammad Najeeb Ahmad, Laurent Vanoye, and Farid Aiouache*

Queen's University of Belfast, School of Chemistry and Chemical Engineering, BT9 5AG, Northern Ireland

ZSM-5 zeolite in H^+ form with an average pore size of 1.2 nm was used for aqueous phase dehydration of xylose to furfural at low temperatures; that is, from 413 to 493 K. The selectivity in furfural increased with the temperature to a value of 473 K. Beyond this temperature, condensation reactions were significant and facilitated by the intrinsic structure of ZSM-5. A reaction mechanism that included isomerization of xylose to lyxose, dehydration of lyxose and xylose to furfural, fragmentation of furfural to organic acids, oligomerization of furfural to bi- and tridimensional furilic species, and complete dehydration of organic acids to carbonaceous deposits was developed, and the associated kinetic parameters were estimated. The rate of furfural production was found to be more sensitive to temperature than the rates of side reactions, with an estimated activation energy of 32.1 kcal/mol. This value correlated well with data in the literature obtained by homogeneous catalytic dehydration.

1. Introduction

With increasing concern about global warming and dwindling oil supplies, attention is turning to "green: processes that use sustainable and environmentally friendly feedstocks. First generation biofuel, which was hailed as a potential source for fuels and products, is progressively facing controversy and hot debate on "fuel vs food". However, second generation biofuels based on lignocellulosic material in the form of waste from biomass such as vegetable peelings, scrap wood, and paper are regarded more favorably as they are carbon dioxide neutral sources with a reduced impact on the food economy.[1] They have a great potential to become the largest feedstock to value added chemicals, such as monosaccharides, via the acid hydrolysis process.[2]

In 2005, world production of furfural was 250 000 tons, and moreover, the catalytic conversion of monosaccharides, such as xylose to furfural via dehydration, has attracted extensive research from academia and industrial sectors during the past decade.[3] Furfural is a useful chemical intermediate mainly used as a solvent for chemical refining and resin synthesis in the petrochemical and automotive industries. Early research in furfural production from biomass concentrated on the use of mineral acids as catalysts. Antal et al.[4] investigated the mechanism of xylose dehydration by using homogeneous sulfuric acid at high temperature (523 K) and high pressure (above 300 bar), with a maximum yield of 60% in furfural. The authors suggested a reaction mechanism where furfural would be produced via an acid-catalyzed anhydride intermediate step. Side reactions were also found to be taking place in the liquid phase and leading to undesirable products such as pyruvaldehyde, formic acid, and lactic acid. The overall reaction scheme included rapid decomposition of the open chain xylose by parallel pathways. The first pathway forms glycolaldehyde, pyruvaldehyde, and fragmentation products such as organic acids, while through the second pathway a xylopyranose ring form reacts to 2,5 anhydride of xylose which further dehydrates to furfural.

Dias et al.[5] used a relatively low temperature of 473 K, moderate pressures, heterogeneous acid catalysts (i.e., surfactant-templated micromesoporous silica, cesium salts of 12-tungstophosphoric heteropolyacids [HPAs]), and a range of solvents such as dimethyl sulfoxide (DMSO), toluene, and isomethylbutyl ketone (IMBK). The group achieved their highest yield in furfural, over 60%, when using HPAs and a temperature of 513 K. Furfural yield was promoted by temperature, catalyst mass, and xylose concentration. In agreement with Antal's work,[4] the reaction rate for the disappearance of xylose was found to be first-order. Product inhibition was attributed to the consumption of protons by Bronsted-base furfural to produce protonated furfural. Both xylose conversion and selectivity to furfural were higher in DMSO than in water-containing solvent systems. According to the authors, the high selectivity was due to a promoted dissociation of protons in polar solvents and reduced condensation of furfural in aqueous−organic medium as it transferred rapidly to the organic phase as soon as it was produced.

Moreau et al.[6] used a variety of zeolites, namely H-form faujasites and mordenites, with several solvents such as water, methyl isobutylketone, and toluene for the dehydration of xylose to furfural. Selectivities above 90% were achieved when structured bidimensional mordenites were used. Xylose could access the catalytic site within the large channel of the pore, and once formed, the furfural could rapidly diffuse out of the pore and into the bulk liquid phase. However, the presence of the larger cavities in the faujasite system allowed further rearrangement and oligomerization of furfural once formed. The promotion of furfural losses in the tridimensional structure of the faujasite system led to relatively low selectivities in furfural.

The importance of the shape and structure of zeolites was reiterated in the work of Lima et al.[7] A delaminated version of the Nu-6 zeolite, which had a surface area about seven times greater than that of standard Nu-6 zeolite, was prepared and tested in a water−toluene biphasic reactor system. The reaction rate was found to be twice as high as that associated with the H-Nu-6 zeolite. The delaminated zeolites share acid properties and stability associated with zeolites but exist as single crystalline sheets with more accessible active sites. The yield in furfural was about 50% at a reaction temperature of 453 K.

The importance of reactant dimensions relative to catalyst pore size was highlighted by Lourvanij et al.,[8] who used glucose

* To whom correspondence should be addressed. E-mail: f.aiouache@qub.ac.uk. Phone: (+44) 2890974065. Fax: +44 (0) 28 90974627.

10.1021/ie801599k CCC: $40.75
Published on Web 04/09/2009

dehydration over Y zeolite. Several secondary reactions were identified, including isomerization of glucose to fructose, partial dehydration of glucose to 5-hydroxymethyl furfural (HMF), rehydration and cleavage of HMF to formic acid and 4-oxo-pentanoic acid, carbonization to form coke, or oligomerization of HMF. The selectivity associated with Y zeolites was found to be lower than that associated with homogeneous catalysts due to molecular sieving reactions that take place within the zeolite. In agreement with the study of Moreau et al.,[9] the author suggested that glucose would have threaded into the zeolite cage and reacted on the Bronsted acid sites. The new forms of the bulky furfural molecules would thereafter be trapped in the zeolite pores and unable to thread out of the cage to the liquid phase.

The aim of this work is to investigate the dehydration of xylose to furfural catalyzed by ZSM-5 zeolite in H^+ form at low temperatures (413−493 K). Commercial ZSM-5 zeolites present a highly uniform three-dimensional structure, and the pore sizes are suitable for xylose and furfural molecular sizes. The structure of the zeolite should allow xylose easy access to the active sites. The products thread out rapidly to the liquid phase with a minimum residence time for condensation and oligomerization reactions in the bulky phase of the pores. H-ZSM-5 zeolite is highly acidic as it contains a high silica to alumina ratio. This study is carried out in a batch reactor where the conditions are varied as follows: initial reactant concentration up to 20 wt % and catalyst to xylose ratio from 0.06 to 0.46 $g_{catalyst}/g_{xylose}$. The suitable conditions for maximum yield of furfural are presented. The reaction mechanism and a kinetic model are proposed.

2. Experimental Details

2.1. Catalyst. The catalyst precursor NH_4-ZSM-5 zeolite was obtained from Johnson Matthey Ltd., UK, in its ammonium form. The precursor was converted to catalyst (H^+ form) by heating at 500 K in air for 820 min. The Si/Al ratio of 28 was measured by inductively coupled plasma-atomic emission spectroscopy (ICP-AES). Catalyst total acid content was determined to be 1.6 ± 0.16 equiv H^+/g using ammonia-temperature programmed desorption (A-TPD) analysis. An amount of ZSM-5 was pretreated under an argon atmosphere for 1 h at 573 K. The catalyst was then cooled down to 303 K, and a mixture of NH_3/argon at 1.0 vol % was introduced for 1 h. Following NH_3 adsorption, the catalyst was purged with argon at 50 cm^3/min for 2 h to remove any weakly bounded ammonia. Finally, the temperature was ramped under argon flow at a rate of 10 K/min up to 973 K. Desorbed species were monitored by a quadrupole mass spectrometer (Hiden Analytical Ltd.). The total desorbed ammonia for an amount of 50 mg of catalyst was found to be 8.3×10^{-5} mol, which implied that 1.6 mmol of NH_3 had been desorbed per gram of catalyst. These acid sites can be divided into two main types according to the two peaks seen on the desorbtion profile: weak acids (0.9 mmol H^+ equiv; NH_3 desorbs between 373 and 473 K) and strong acids (0.7 mmol H^+ equiv; NH_3 desorbs at temperatures greater than 673 K). Therefore, the total acidity was 1.6 mmol H^+ equiv/g, and this is the value which shall be used in later calculations. Using liquid N_2 adsorption from ASAP 2010 (Micrometrics), the three-parameter Brunauer−Emmet−Teller (BET) method was used to calculate the average pore size of the catalyst. Assuming a cylindrical geometry of the pores, a value of 1.2 nm was obtained. This value does not represent the effective pore size of H-ZSM-5 but represents an estimate of the average pore size, reflecting the contribution of the external surface to the total surface (internal plus external). The high value of the pore size could indicate the coexistence of two phases: one crystalline with microporous characteristics and the other with more open porosity.

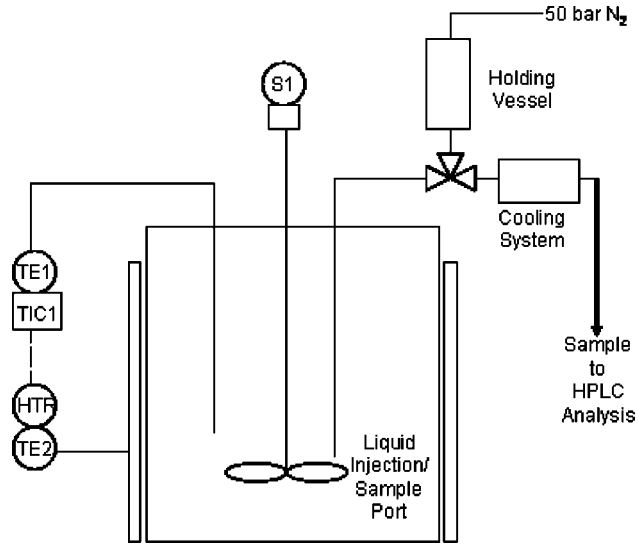

Figure 1. Experimental setup. HTR = heating jacket, TE2 = thermocouple for the heating jacket, T1C1 = temperature indicator controller of the heating jacket, TE1 = thermocouple temperature inside the reactor, S1 = stirrer.

2.2. Batch Reactor. The experiments were carried out in a modified 100 mL, four port, stainless steel autoclave reactor (Autoclave Engineers, USA) as shown in Figure 1. The four ports allowed inserted thermocouples to be digitally linked to a computer for fast data collection, a pressure relief valve to maintain constant pressure during product sampling, a needle valve for gas phase sampling, and a second needle valve for liquid phase sampling. The liquid sampling valve allowed liquid samples to go both in and out of the reactor. This valve was attached to a threaded piece of 1/8 in. tubing which sat below the liquid level, enabling samples to be obtained from the liquid phase. The reactor was attached to a 50 mL stainless steel sampling vessel which was connected to a supply of helium at 50 bar pressure. This additional setup allowed xylose solution to be held at room temperature until the reactor reached the desired temperature, at which time xylose solution was charged to the reactor. This procedure minimized the initial degradation of xylose before starting the reaction. The reaction mixture was stirred using a six-blade turbine stirrer, which was also digitally linked to a computer. The reactor was heated with an external jacket with an on/off temperature control and a precision of 3 K.

2.3. Procedure. Xylose, prepared catalyst, and distilled water were weighed separately to a precision of 1%. The catalyst along with approximately 80% of the total amount of required water was placed in the reactor and stirred at 800 rpm. The reactor was then purged, pressurized to around 30 bar using helium, and heated to the desired temperature. Xylose was dissolved in the remaining water and injected into the sampling vessel. When the desired temperature was reached, the solution of xylose was charged to the reactor using helium as an entrainer at 50 bar pressure. Initial liquid samples were taken every minute and then less frequently as the reaction continued. The liquid samples were stored in an ice bath, diluted, and sent for analysis by high-performance liquid chromatography (HPLC).

2.4. Analysis. Liquid samples were analyzed by HPLC using a method described elsewhere.[10] In the course of the reaction,

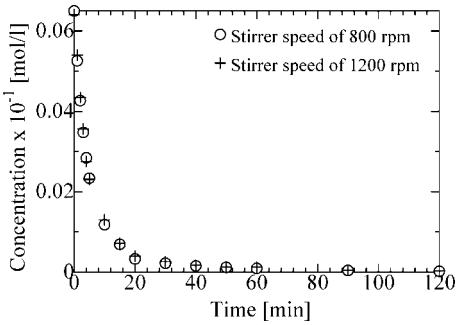

Figure 2. Xylose degradation at 473 K, stirrer speed of 800 and 1200 rpm, and under standard conditions.

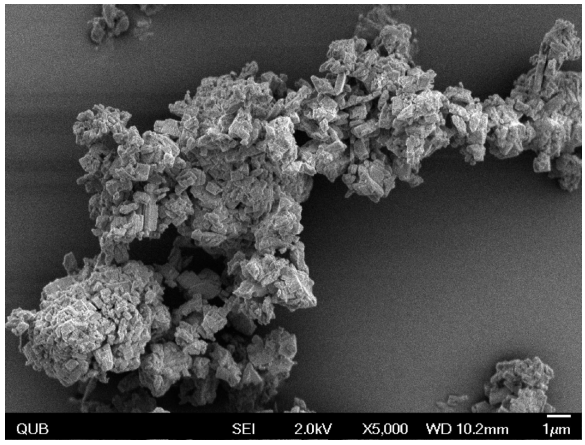

Figure 3. Scanning electron micrograph of catalyst particle.

the catalyst was often found coated by a black solid. This solid layer was further analyzed using a variety of techniques including CHN analysis, thermogravimetry analysis (TGA), and electron ionization (EI) analysis.

3. Results

Directed by preliminary experiments on the effect of mass transfer on reaction kinetic profiles, a stirring speed of 800 rpm was selected. Beyond this value, the external mass transport resistance was found to be negligible in the microporous zeolite, as shown in Figure 2. The internal mass transfer resistance was considered negligible as the size of catalyst particles determined by SEM was micrometers in range, as shown in Figure 3. Under standard conditions, a solution of xylose of 10 wt % and ratio of catalyst to xylose of 0.3 (w/w) were used. The analysis by HPLC revealed the following products: furfural, organic acids such as formic acid, and lyxose, which is an isomer of xylose.

3.1. Effect of Time.

3.1.1. Liquid Phase Component Profiles. The evolution of furfural, lyxose, and organic acids in the course of a reaction under standard conditions and temperature 473 K is shown in Figure 4. The reaction products identified by HPLC analysis were furfural, lyxose, and formic acid. The reaction initially began with high rates of conversion of xylose to lyxose and furfural. As the reaction progressed, lyxose reached a maximum value and then decreased while more furfural was formed. Furfural followed a similar trend to lyxose, reaching a maximum value, and then decreasing as organic acids evolved. It is interesting to notice that the mass balance was not conserved in the liquid phase. A part of the products adsorbed on the catalyst formed solids and were therefore lost from the liquid phase (the solid deposit mechanism will be discussed in section 3.1.2). Eventually all water-soluble products disappeared as the solid yield continually increased as all products underwent carbonization.

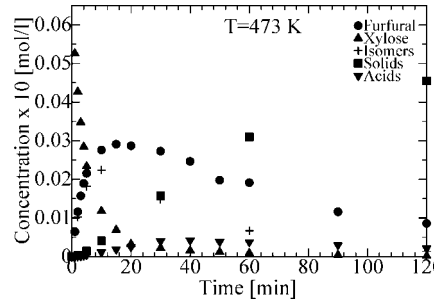

Figure 4. Concentration profiles of reaction products: $T = 473$ K, xylose concentration in water = 10 wt %, and ratio of catalyst to xylose of 0.3 (w/w).

Under standard conditions, the selectivity to furfural was initially high and remained relatively high for a period of approximately 30 min, although most of the xylose was converted within the initial 18 min. This was due to the fact that furfural was produced not exclusively from xylose, but from lyxose as well. Furfural production from lyxose tends to be slower than production from xylose; therefore the selectivity remained quite high for a relatively long period of time. After a period of 30 min, the selectivity to furfural decreased, as both the fragmentation reaction to produce short chain organic acids and the condensation reaction to produce oligomers increased, leading to an increase in the solid formation.

3.1.2. Solid Phase Component Profiles. A dark brown solid evolved throughout the reaction. This solid residue caused the catalyst to become discolored. To determine the mass of solid, the reaction had to be repeated and rapidly quenched after a set amount of time. The reaction was quenched by simultaneously injecting cold water into the reactor and plunging the reactor into an ice bath. This gave a temperature drop of approximately 50 K in less than 20 s. The solid residue was separated from the liquid phase, dried in a vacuum oven, and weighed. The samples were then placed in a Q5000 TGA equipped with a platinum plate. The system was made inert by flowing nitrogen gas and the temperature was increased to 1073 K. The decrease in catalyst mass was measured using an internal microbalance and identification was made possible by using electron ionization (Waters GCT EI machine). The main peak corresponded to oligomers of furfural originating from furfural oligomerization reactions. The oligomerization of furfural in acidic faujasite zeolites (H-Fe-FAU) has been studied by Roque-Malherbe et al.,[9] who demonstrated that the aldolic condensation of furfural forms two- and three-dimensional furilic (T-T-DF) species. The smaller peaks indicated a complete dehydration of furfural and organic acids to carbonaceous solids. It was thought that the organic acid formed throughout the reaction may react with furfural and this may contribute to the formation of solids. However, further studies proved that this was not the case at such low organic acids concentrations. It can be seen from Figure 4 that within the first 20 min of the reaction, when the xylose concentration was high, the solid yield was negligible, and the solids concentration increased dramatically once the furfural concentration declined. This indicates that the xylose was not directly involved in the formation of solids. Also, we confirmed this result by carrying out an additional reaction between formic acid and furfural at 473 K. During an hour of the reaction course, no noticeable change in reactant concentrations or solid deposit was observed.

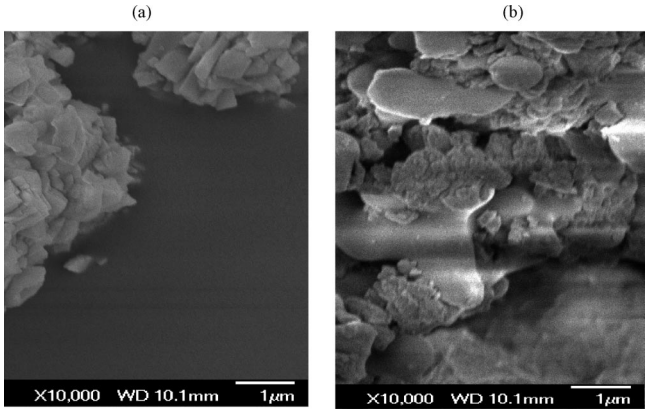

Figure 5. Scanning electron micrograph of H-ZSM-5 catalyst fresh (a) and used (b).

The black deposits found on the catalyst can be explained as follows; the average pore diameter of ZSM-5 measured by BET analysis was 1.2 nm. The approximate molecular diameters of xylose and furfural were estimated by using a commercial software package, CambridgeSoft, USA. Along the longest axis, they were found to be 0.68 and 0.57 nm, respectively, and in accordance with literature.[10] The relatively large pore size would allow furfural to have a longer residence time within the catalyst. This would allow rearrangements of furfural to form oligomer, with the furanic ring breaking cleaving and allowing the formile group to take part in addition reactions. Once formed, these larger molecules would not be able to move freely in and out of the pores and, ultimately, would get trapped in the pore framework.

In order to look at various sources of catalyst deactivation, postexperiment analysis of the catalyst morphology was carried out. The SEM of fresh and used catalysts with a higher magnification than Figure 3 are shown in Figures 5a and b, respectively. Figure 5a shows tightly aggregated nanoparticles of 0.5−1 μm size, with regular shape, straight angles, and little amorphous impurities. Figure 5b shows partial coating of nanoparticle surfaces by oligomer deposits and narrow openings of catalyst pores to reactive species. These results demonstrate that the main source of catalyst deactivation is the solid residue from furfural oligomerization.

3.2. Effect of Temperature. The reaction temperatures studied were 413, 433, 453, 473, and 493 K. The working temperatures were highly influential in the distribution of products as shown in Figure 6. At low temperatures, namely 413−433 K, the isomer of xylose (lyxose) was more prominent, accounting for the majority of the products throughout the reaction. Lyxose is known to form rapidly from open chain xylose and disappears slowly to form furfural. As the temperature increased the rate of formation of furfural from lyxose increased. Organic acid yields were negligible at low temperatures and solid phase species were very low. Acid formation increased with temperature but was unstable and degraded to solid species quickly. The maximum achievable yield in furfural increased with temperature, which reveals the positive effect of temperature on xylose dehydration to furfural. At elevated temperatures, however, furfural was highly unstable and degraded more quickly: for instance at a temperature of 493 K, furfural had degraded to half of its maximum value after 10 min.

Solids production increased at increasing temperatures. However, conversion also increased at higher temperatures, and therefore, it is incorrect to compare the solids production at a set time; instead, it should be compared at set conversions. The optimum temperature for maximum yield with minimum solids production is 473 K.

3.3. Reaction Mechanism and Kinetics Model. 3.3.1. Reaction Mechanism. By analogy with the glucose dehydration pathway proposed by Lourvanij et al.,[8] the xylose dehydration mechanism is illustrated in Figure 7. The reaction will follow a series of elementary steps which will involve the liberation of three molecules of water per xylose molecule and two main side reactions that will lead to organic acids and solid species.

Xylose molecules in the liquid phase pass into the catalyst and adsorb onto the acidic active site of ZSM-5. The acidic sites catalyze the reversible isomerization reaction of xylose to lyxose (steps 1 and 2). The isomerization occurs through the formation of the linear open chain of xylose molecules caused by the acid-catalyzed hydrolysis of the hemi acetyl which results in cleavage of the C−O bond between carbon 1 and oxygen 5. Alternatively, xylose molecules undergo a complex dehydration step by losing three molecules of water and forming furfural (step 3). The liberation of the water molecules from xylose begins with the protonation of oxygen 2, followed by a loss of a water molecule from carbon 2; oxygen 5 then attacks the resulting carbocation, and as a result, an additional two water molecules are lost.[11]

Also, lyxose molecules dehydrate partially in a similar way to xylose by losing three water molecules to form furfural (step 4). Furfural molecules either desorb, pass out of the zeolite pores and diffuse into the liquid phase, leading to furfural in the liquid phase, or degrade and fragment to form organic acids (step 5). Furfural molecules form oligomers inside the porous network of ZSM-5 (step 6). Furfural reacts through the furanic ring and the formile group. The furanic ring gets broken and the formile group takes part in addition reactions, forming T-T-DF species.[9] The suggested structure of these oligomers shown in Figure 7 was adapted from the work of Clayden et al.[12] The broken furanic ring bonds to a cyclic furfural and forms a short chain oligomer with a large number of double bonds. The highly reactive double bonds undergo further addition reactions to form longer chain furfural oligomers. These oligomers have large molecular diameters and cannot easily thread out of the pore network back into the liquid phase and, therefore, form solid deposits on the catalyst. The organic acids dehydrate completely to form carbonaceous solids on the zeolite surface (step 7). A portion of furfural trapped in the zeolite pores threads out and rejoins the liquid phase (step 8).

The formation of degradation products such as formic acid and oligomers of furfural highlights the importance of the course time for this reaction. As furfural is the desired product, its decomposition to both formic acid and carbonaceous deposit is detrimental to the reaction.

3.3.2. Kinetics Calculations. The kinetics of dehydration of xylose was estimated based on an initial reaction of xylose dehydration for various concentrations of xylose and acid concentrations. Xylose concentration was varied from 10 to 20 wt %, and catalyst concentrations varied from 0 to 30 $g/L_{solution}$, as shown in Figure 8. From this graph, it is clear that the xylose dehydration rate is proportional linearly to both acid concentration and initial concentration of xylose. This would leave a monomolecular kinetic model of the surface mechanism of xylose for each acid site of ZSM-5 zeolite. As with the dehydration of glucose,[8] the mechanism of xylose dehydration fits a first order kinetic model well. Moreover, the intersection of the curve with the coordinate

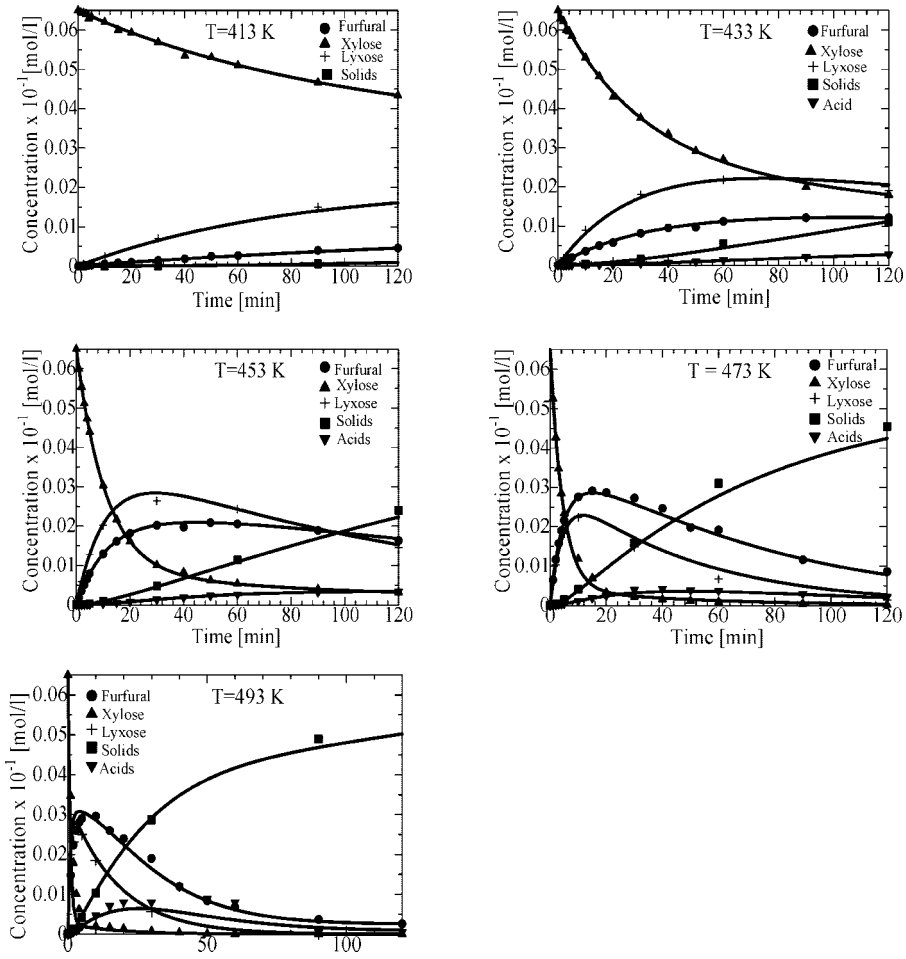

Figure 6. Concentration profiles of reaction products at various temperatures. The solid black lines indicate the simulation results: xylose concentration in water = 10 wt % and ratio of catalyst to xylose of 0.3 (w/w).

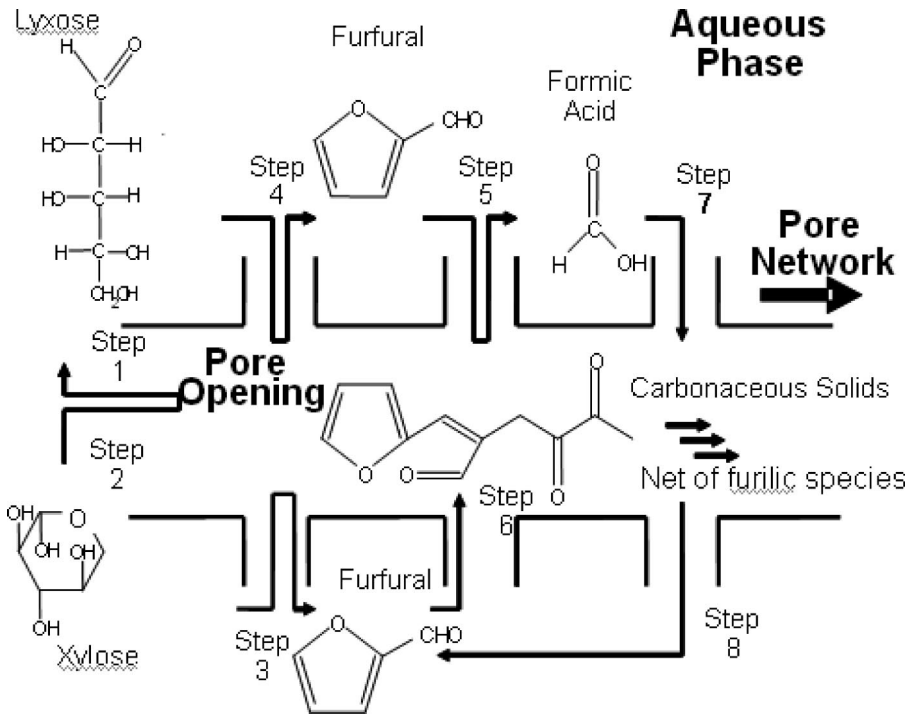

Figure 7. Simplified reaction scheme for the dehydration of xylose.

axis demonstrates that this reaction may occur without the addition of a catalyst. This autocatalysis is attributed to thermal degradation of xylose which leads to production of organic acids. The organic acids, in their turn, promote

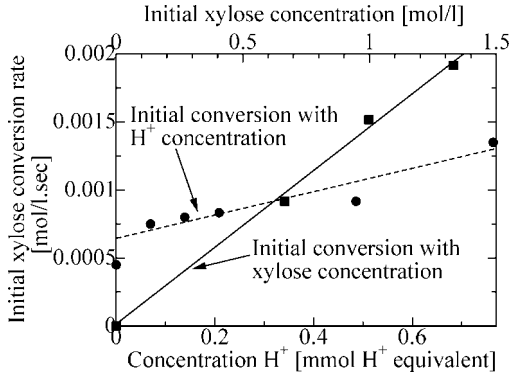

Figure 8. Initial xylose conversion at 473 K as a function of the initial concentration of xylose (a) at a ratio of catalyst to xylose of 0.3 (w/w) and loaded acidity (b) at a xylose concentration in water = 10 wt %.

homogeneous catalysis which will then go on to catalyze the reaction. Similarly to the results of Dias et al.,[13] the conversion rate and selectivity (graphs not shown) were greatly reduced when no catalyst was present. This would indicate that solid acid catalyst promoted the dehydration of xylose into furfural.

A surface kinetic model with a first-order mechanism was considered. The validity of the model was tested by fitting the proposed rate equations to the experimental data. The reaction rate of component *i*, r_i, based on one proton can be written as follows:

$$r_i = \frac{\mathrm{d}n_i}{m_{\mathrm{cat}} Q_{\mathrm{cat}}\, \mathrm{d}t} \tag{1}$$

When eq 1 is applied to each component, it yields the following equations

$$r_{\mathrm{xylose}} = -k_1\vartheta_{\mathrm{xylose}} - k_3\vartheta_{\mathrm{xylose}} + k_2\vartheta_{\mathrm{lyxose}} \tag{2}$$

$$r_{\mathrm{furfural}} = k_3\vartheta_{\mathrm{xylose}} + k_8\vartheta_{\mathrm{T\text{-}T\text{-}DF}} + k_4\vartheta_{\mathrm{lyxose}} - k_6\vartheta_{\mathrm{furfural}} - k_5\vartheta_{\mathrm{furfural}} \tag{3}$$

$$r_{\mathrm{lyxose}} = k_1\vartheta_{\mathrm{xylose}} - k_2\vartheta_{\mathrm{lyxose}} - k_4\vartheta_{\mathrm{lyxose}} \tag{4}$$

$$r_{\mathrm{acids}} = k_5\vartheta_{\mathrm{furfural}} - k_7\vartheta_{\mathrm{acids}} \tag{5}$$

$$r_{\mathrm{T\text{-}T\text{-}DF}} = k_7\vartheta_{\mathrm{acids}} + k_6\vartheta_{\mathrm{furfural}} - k_8\vartheta_{\mathrm{T\text{-}T\text{-}DF}} \tag{6}$$

The coverage of component *i*, θ_i is expressed by a pseudolinear adsorption model. This linear model is considered because of the high dilution of the components in the aqueous solution.

$$\theta_i = K_i C_i \tag{7}$$

where K_i is the adsorption constant of the component *i* and C_i is the concentration of component *i* in the liquid phase. Therefore, reaction rate eqs 2−6 become

$$r_{\mathrm{xylose}} = -k_{f1}C_{\mathrm{xylose}} - k_{f3}C_{\mathrm{xylose}} + k_{f2}C_{\mathrm{lyxose}} \tag{8}$$

$$r_{\mathrm{furfural}} = k_{f3}C_{\mathrm{xylose}} + k_{f8}C_{\mathrm{T\text{-}T\text{-}DF}} + k_{f4}C_{\mathrm{lyxose}} - k_{f6}C_{\mathrm{furfural}} - k_{f5}C_{\mathrm{furfural}} \tag{9}$$

$$r_{\mathrm{lyxose}} = k_{f1}C_{\mathrm{xylose}} - k_{f2}C_{\mathrm{lyxose}} - k_{f4}C_{\mathrm{lyxose}} \tag{10}$$

$$r_{\mathrm{acids}} = k_{f5}C_{\mathrm{furfural}} - k_{f7}C_{\mathrm{acids}} \tag{11}$$

$$r_{\mathrm{T\text{-}T\text{-}DF}} = k_{f7}C_{\mathrm{acids}} + k_{f6}C_{\mathrm{furfural}} - k_{f8}C_{\mathrm{T\text{-}T\text{-}DF}} \tag{12}$$

where

$$k_{fj} = K_i k_j \tag{13}$$

Reaction rate expressions were numerically integrated by using a Rung−Kutta algorithm with a self-adjusting step. The minimization of the sum of squares of residuals was performed by the "nonlinear least-squares method", using the Marquardt method to adjust the kinetic parameters. The changes in the kinetic constants with temperature are illustrated in Figure 9. The validity of the kinetic model was verified by calculating the normalized standard deviation (NSD) as expressed by eq 14:

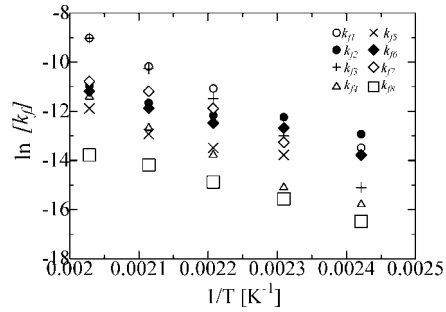

Figure 9. Rate constant changes with temperature: xylose concentration in water = 10 wt % and ratio of catalyst to xylose of 0.3 (w/w).

Table 1. Rate Constant Changes with Temperature According to Arrhenius Expression: $k_{fj} = A_j \exp(E_j/RT)$[a]

k_{fj}	A_j (m^3/(mol H^+ s))	E_j (kcal/mol)
k_{f1}	1.4×10^4	23.3
k_{f2}	2.6×10^3	9.5
k_{f3}	5.9×10^7	32.1
k_{f4}	1.4×10^3	23.5
k_{f5}	5.9×10^{-2}	13.7
k_{f6}	5.1×10^{-2}	12.6
k_{f7}	2.3×10^{-1}	18.2
k_{f8}	2.6×10^{-2}	14.5

[a] Normalized standard deviation (%): furfural 3.4; xylose 6.7; lyxose 6.4; solid 4.5; and acids 11.5.

$$\mathrm{NSD}\ (\%) = 100\sqrt{\frac{\left(\sum_{i=1}^{n}\frac{(c_{\mathrm{exp},i} - c_{\mathrm{calc},i})}{c_{\mathrm{exp},i}}\right)^2}{n-1}} \tag{14}$$

where *n* is the number of data points.

Table 1 illustrates kinetic constant values and the NSD of the actual component concentrations and those obtained from the kinetic model. With the exception of acid, the NSD of components did not exceed 6.5%. The high value of NSD for acids (11.5%) would be due to the low amounts obtained along the reaction course, as shown in Figure 6.

Figure 6 shows the simulated results under standard conditions. The surface model with first-order kinetics for each step in the overall mechanism fits well with the experimental data. The Arrhenius expression gave a good fit to the rate constants obtained. As illustrated in Figure 9, the best correlation coefficient R^2 was achieved by the rate constant of xylose dehydration k_{f1} with a value higher than of 0.998, while the lowest R^2 was achieved by k_{f5} with a value higher than 0.93. The rate of furfural production is more sensitive to temperature than the rates of other reaction steps, as shown by the corresponding activation energy of 32.1 kcal/mol in Table 1. This value correlates well with the 34 kcal/mol obtained by Antal et al. using sulfuric acid.[4] Also, lyxose is more resilient to dehydration than xylose, as its corresponding rate constant k_{f4} is lower than that of xylose k_{f3}. The rate constant k_{f8} is very small relative to the sum of rate constants k_{f6} and k_{f7}. This result is confirmed by the high accumulation of solid species.

4. Conclusion

The dehydration of xylose to furfural in aqueous solutions by ZSM-5 zeolite catalyst was studied in a temperature range of 413−493 K. The average pore size of about 1.2 nm of the ZSM-5 catalyst was found to be far greater than the molecular diameter of both the reactant and the products. The large internal pore area allowed furfural molecules enough time to congregate and react with each other to oligomerize and form T-T-DF molecules. Therefore, a zeolite with a smaller pore size and ideally close to xylose and furfural molecular sizes, for example around 0.8 nm, would be more effective for the dehydration of xylose to furfural, as it would allow enough room for xylose to thread in and dehydrate to furfural. Furfural in turn could desorb and pass out of the pore with ease. A kinetic model was developed and based on a complex reaction pathway that includes the isomerization of xylose to lyxose, dehydration of lyxose and xylose to furfural, rehydration of furfural to organic acids, oligomerization of furfural to T-T-DF oligomers, and complete dehydration of organic acids to carbonaceous deposits. The rate of furfural production was found to be more sensitive to temperature increase than the rates of other reaction steps. A first order kinetic model with an activation energy of 32.1 kcal/mol was observed. A suitable temperature was found to be 473 K, where a balance between the rate of formation of furfural and rate of degradation of furfural to T-T-DF oligomers and formic acid was achieved. At this temperature a yield of 46% furfural was obtained.

Nomenclature

A_j = frequency factor (m^3/(mol H^+ s))
E_j = activation energy (kJ/mol)
k_{fj} = reaction rate constant (m^3/(mol H^+ s))
K_i = adsorption equilibrium constant of species i (m^3/mol)
k_j = reaction rate constant (mol/(mol H^+ s))
m_{cat} = mass of the catalyst (kg)
n_i = mole number of species i in the liquid phase (mol)
Q_{cat} = acidity of the catalyst (mol H^+/kg)
r_i = reaction rate of species i (mol/(mol H^+ s))
t = time (s)
θ_i = surface coverage of the species i, dimensionless

Chemical Species

HPAs = 1,2-tungstophosphoric heteropolyacids
DMSO = dimethyl sulfoxide
IMBK = isomethylbutyl ketone
HMF = 5-hydroxymethyl furfural
(T-T-DF) = two- and tridimensional furilic

Abbreviations

ICP-AES = inductively coupled plasma-atomic emission spectroscopy
A-TPD = ammonia-temperature programmed desorption
HPLC = high-performance liquid chromatography
TGA = thermogravimetry analysis
EI = electron ionization

Literature Cited

(1) Huber, G. W.; Iborra, S.; Corma, A. *Chem. Rev.* **2006**, *9*, 4044–4098.
(2) Orozco, A.; Ahmad, M.; Rooney, D.; Walker, G. *Process Safety Environ. Prot.* **2007**, *5*, 446–449.
(3) Tin Win, D. *Au J. Technol.* **2005**, *4*, 185–190.
(4) Antal, M. J.; Leesomboon, T.; Mok, W. S.; Richards, G. N. *Carbohydr. Res.* **1991**, 71–85.
(5) Dias, A. S.; Pillinger, M.; Valente, A. A. *J. Catal.* **2005**, *2*, 414–423.
(6) Moreau, C.; Durand, R.; Peyron, D.; Duhamet, J.; Rivalier, P. *Ind. Crops Products* **1998**, *2*−*3*, 95–99.
(7) Lima, S.; Pillinger, M.; Valente, A. A. *Catal. Commun.* **2008**, *11*−*12*, 2144–2148.
(8) Lourvanij, K.; Rorrer, G. L. *J. Chem. Technol. Biotechnol.* **1997**, *1*, 35–44.
(9) Malherbe, R. R.; De Onate-Martinez, J.; Navarro, E. *J. Mater. Sci. Lett.* **1993**, *13*, 1037–1038.
(10) Sjöman, E.; Mänttäri, M.; Nyström, M.; Koivikko, H.; Heikkilä, H. *J. Membr. Sci.* **2007**, *1*−*2*, 106–115.
(11) Nimlos, M. R.; Qian, X.; Davis, M.; Himmel, M. E.; Johnson, D. K. *J. Phys. Chem. A* **2006**, *42*, 11824–11838.
(12) Clayden, J.; Warren, S.; Greeves, N.; Wothers, P. Reactions of enolates with aldehydes and ketones: the aldol reaction. In *Organic Chemistry*; Oxford University Press: New York, 2000; pp 691−694.
(13) Dias, A.; Pillinger, M.; Valente, A. *Appl. Catal. A: Gen.* **2005**, *1*−*2*, 126–131.

Received for review October 22, 2008
Revised manuscript received March 2, 2009
Accepted March 17, 2009

IE801599K